



Nanoparticle prepared mechanically stable hierarchically porous Silica granulates and their application as Oxygen Carrier Supports for Chemical Looping Combustion

Journal:	<i>Journal of Materials Chemistry A</i>
Manuscript ID:	TA-ART-03-2015-001842.R1
Article Type:	Paper
Date Submitted by the Author:	15-Apr-2015
Complete List of Authors:	Liu, Yujing; Empa, the Swiss Federal Laboratories for Materials Science and Technology, Kirchesch, Peter; Empa, the Swiss Federal Laboratories for Materials Science and Technology, ; Hochschule Koblenz, Department of Materials Engineering, Glass and Ceramics Graule, Thomas; Empa, the Swiss Federal Laboratories for Materials Science and Technology, Liersch, Antje; Hochschule Koblenz, Department of Materials Engineering, Glass and Ceramics Clemens, Frank; EMPA, Laboratory for High Performance Ceramics

Nanoparticle prepared mechanically stable hierarchically porous Silica granulates and their application as Oxygen Carrier Supports for Chemical Looping Combustion

Yujing Liu^{1*}, Peter Kirchesch^{1,2}, Thomas Graule¹, Antje Liersch², Frank Clemens^{1*}

¹Laboratory for High Performance Ceramics, Swiss Federal Laboratories for Materials Science and Technology, EMPA, Switzerland; ²Department of Materials Engineering, Glass and Ceramics, Hochschule Koblenz, Germany.

Abstract

Chemical looping combustion (CLC) represents a promising approach to capture CO₂ emissions in the fossil fuel powered energy generations. Oxygen carriers, composed of active metal oxides, play important roles in CLC process by transferring oxygen between oxidation and reduction reactors. To avoid the agglomeration of metallic phase during the reduction process and ensure a long-term activity, a porous support granulate is highly required. In this work, we proposed a bottom-up strategy to fabricate mechanical stable hierarchical porous granulates from silica nanoparticles, via the integration of soft pore former Pluronic F127 and employment of cold isostatic pressing technique. According to this strategy, the developed silica granulates possess characteristics such as mesopore (ca. 33 nm) and macropore (ca. 175 nm) combined hierarchical porous structure, high pore volume (955 mm³/g) and surface area (114 mm²/g), as well as enhanced crushing force 1.94 N. Via the dry impregnation method, fully oxidized CuO was able to be loaded on the surface of porous granulates and a loading amount of 30 wt.% was obtained after repeating the impregnation process only twice. Further simulated chemical looping tests revealed that, with the similar loading amount, CuO supported on developed silica granulate shows a higher oxygen transport capacity comparing with reference work.

1. Introduction

In the next few decades, combustion of conventional fossil fuels will keep playing important roles in the existing energy supplying system. One of the direct consequences of fossil fuel combustion is CO₂ emission, the source which brings disastrous impacts on climate change and other greenhouse gas effects [1-3]. Technologies to capture CO₂, such as solvent scrubbing of the exhaust gas, or alternative combustion process with gas mixture (O₂ and CO₂) have been investigated[4]. However, the main drawbacks of these methods are the reduction of power generation efficiency (e.g., the energy penalty for amine scrubbing is ca. 10 %) [4-6] and extra costly cleaning units are required to remove impurities like SO_x and NO_x from the exhausts. Chemical looping combustion, presents a very promising option to achieve efficient reduction of CO₂ emission from fossil fuel-fired plants, has been proposed [7-9]. Different from the conventional combustion methods, the chemical looping process avoids the contact between air (mixture of O₂, N₂ and many others) and fuels, while the combustion is completed by the use of an oxygen storage material ‘oxygen carrier’ to provide the required oxygen. Impurities like NO_x and SO_x won’t be generated if no fuel-bound nitrogen is present and costs for CO₂ cleaning can be avoided.

To develop CLC process into practical applications, high performance oxygen carrier material is highly required and its research has attracted a lot of attention over the last decade [3, 10, 11]. Generally, the oxygen carrier materials are composed of transition metal oxides, which have the ability to release free oxygen at high temperature (fuel combustion or self-reduction) and re-gain the lost oxygen in another reactor (air reactor), to realize their regeneration and recyclable long term use. To avoid the agglomeration of the reduced metallic phase at high operation temperature and ensure the long-term activity, a porous support material for the active metal oxide is highly suggested [7, 11-16]. For example, de Diego et.al found out that, under the operation temperature 800°C, without support, Cu oxide lost its 90% initial activity after only three cycles of redox process, while no loss could be obviously noticed with the use of a silica support after a multiple cycle test [13].

As supports for active metal oxides, the ideal requirements are lying on their high pore volume and specific surface area to guarantee a high loading amount and well dispersion of metal oxides, open porous microstructure for efficient gas transfer, being inert to the active metal oxide

(chemical stability), and being mechanically stable. Mechanical mixing [17], spray drying [18], wet impregnation [16] and other methods have shown promise in preparing required oxygen carrier materials, however, the mechanical strength of the produced materials in some cases were inferior to practical use needed. There were also research works targeted to improve oxygen carriers mechanical stability [19]. For example, in a recent published work by Peterson et.al. [20], the mechanical stable β -SiC was used as initial hard framework to support active phase CuO, and the obtained oxygen carrier granulates were rather strong, with crushing force above 4 N. However, to convert β -SiC completely to SiO₂, the authors have performed a rather long oxidizing procedure, 980°C for continuous 7 days, and moreover, the obtained support granulates SiO₂ show rather limited porous characteristics, with BET surface area at ca. 10 mm²/g and specific pore volume ca. 64 mm³/g.

In this work, attentions are expected to be paid both onto granulates porous characteristics and their mechanical stability. For the porous characteristics, the plant leaf inspired hierarchically structured porous materials, featuring a combination of varied pore size distributions and emerging themselves for applications in many different applications, such as catalysts, separation, energy conversion and storage devices, as well as life science [21, 22], have attracted our attention. For example, in the case of meso- and macro-pore combined structures, materials will thus have the advantage of mesopores resulted high surface area and large macro-pore facilitated better impregnation in avoiding possible pore blockings, which would be of interest for applications in chemical looping process, where a large surface area and accessible paths for mass transport are needed. However, to the best of our knowledge, research works on the application of these materials to support active metal oxides and use for chemical looping process have not been noticed in the previous publications. The aim of this work is to fabricate hierarchically structured porous granulates, with a combination of pore sizes within the mesopore range (2-50 nm) and macropore range (> 50 nm), and then apply them as the supports for active metal oxides in chemical looping process. As for the enhancement of the mechanical stability of granulates and to ensure a long term use in a dynamic attritional environment, cold isostatic pressing (CIP), the known technique used in structural ceramics processing [23] to achieve higher packing density of raw materials and higher mechanical strength (hardness), would be employed within the procedure to fabricate hierarchical porous granulates.

With these requests in mind, we proposed a strategy to start the fabrication of granulates from small nanoparticles, and tune the microstructure of granulates into hierarchical porous characteristics via the integration of different pore formers and improve granulate mechanical strength via employment of CIP. With the obtained porous granulates, active metal oxide will be impregnated into the porous system and the generated oxygen carriers will be tested for chemical looping applications. Due to the excellent stability of SiO_2 / Cu oxide system [2, 24-26], silica was selected as the support and Cu oxide was selected as active metal oxide for oxygen transfer in this work. Besides, CuO is also a very promising candidate in an alternative CLC process, the chemical looping of oxygen uncoupling process (CLOU), as it showed a combination of high partial pressure of O_2 at relevant low temperature and an exothermic reaction in fuel reactor [27]. Therefore, the investigation on CuO redox behavior on supported silica granulates also posts great interests for CLOU applications.

2. Experimental part

2.1 Nanoparticle agglomeration breakage

Silica nanoparticles used for the preparation of granulates were purchased from Skyspring Nanomaterials (USA), with diameter as 20 nm and surface area as $160 \text{ mm}^2/\text{g}$ (supplier data). When disperse the nanoparticles in water, big agglomerations (ca. 3-5 μm) were unavoidably generated. To achieve well dispersed silica nanoparticles in the water, two different approaches have been applied: the modification of dispersion pH and the employment of mechanical treatments. For the first method, the initial prepared silica dispersion (pH = 7.0) were further modified to pH 5.6, pH 3.7 and pH 2.3 by 1 N citric acid solution, to pH 8.5 and pH 10.0 by 1 N NaOH solution, and laser scattering measurements were performed on these dispersions after 30 min magnetic stirring. For the second method, 30 min mechanical force treatments were applied either via vibrational ball milling or ultra-sonication bath, and the resulted agglomeration size were checked by dynamic light scattering (DLS).

2.2 Preparation of hierarchically porous silica granulates

The fabrication procedure of porous granulates was illustrated in Figure 1. At the beginning of the procedure, 6 g silica nanoparticles were dispersed into 60 ml di-ionized water and stirred overnight on a magnet plate (ca. 500 rpm/min). To obtain granulates with a varied porous structure, different pore formers were integrated into the system in the form of water suspensions,

with the intention to achieve a better miscibility with nanoparticles. The selected pore formers were Pluronic F127 (Molecular weight: 12600 g/mol, real density: 1.10 mm³/g, Sigma-Aldrich) and Carbon black (Acetylene Black P 200 MPa hv, real density of 1.90 mm³/g, SKW Piesteritz GmbH), each with a content of 10 vol.% of 6 g silica nanoparticles. In the case of Pluronic F127, 2.87 mL F127 suspension (10 wt.% in water) was added into 60 mL 10 wt.% nanoparticle suspension; while in the case of Carbon black, an additional surfactant DBSA (Dodecylbenzenesulfonic acid, soft type, 90%, ABCR GmbH, Germany) needs to be used to assist its dispersion in water, and then this well dispersed suspension (4.96 ml, 10 wt.% of Carbon black, with 0.13 g DBSA) was added into 60 mL 10 wt.% nanoparticle suspension. Afterwards, the suspension mixtures were left for stirring for ca. 4 hours and then transferred to an ultra-sonication bath (Bandelin electronic, 35 kHz) for 30 min, to break down big agglomerations formed inside the dispersion.

To get rid of water in the prepared suspensions, vacuum filtration and a controlled drying process at 60 °C was applied, as shown in Figure 1. In this work, vacuum filtration device was composed of a bottom-up filter with pore diameter 0.45 μm and an additional filter membrane (50 nm in diameter, Whatman nuclepore track etched membrane, GE Healthcare Life Science) above the filter, connected with a vacuum pump (DIVAC 1.2 L, vacuum level ca. 1.1×10⁻¹ mPa). After the vacuum filtration process, the paste like green body was collected from the bottom-top filter and further dried at 60°C to remove the additional water. The drying time was controlled according to the required water content. With the obtained green bodies cold-isostatic pressing (CIP, Kalt Isostatische Presse 110-350-200, VITEK N.V.) was applied under the pressure of 50 MPa with a preservation time of 2 min. Then, CIP treated green bodies were immediately put into preheated oven (130 °C), followed by a thermal treatment at 900 °C for 30 min (ramping speed 5 °C/min), with separate stay at 300 °C for 2 hours (0.5 °C/min from room temperature to 300 °C, then 1°C/min to 500 °C). In the end, the thermal treated samples were grinded into smaller pieces and sieved. Granulates with size between 315 μm and 500 μm were selected for next step.

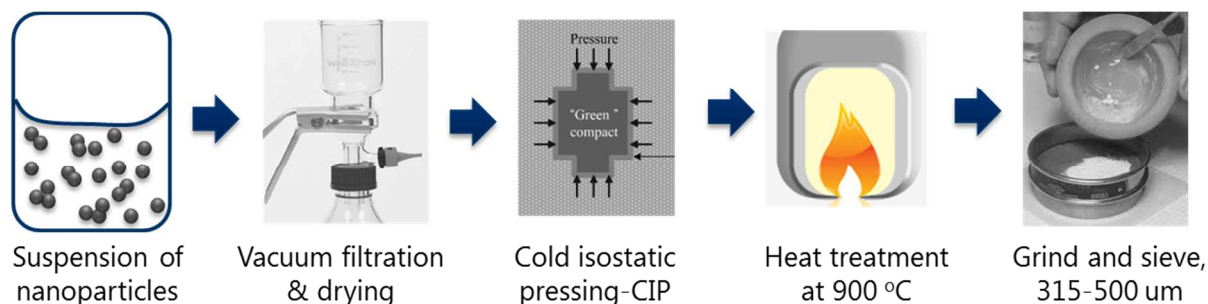


Figure 1. Illustrative flow-chart of granulate preparation procedure: 1) the preparation of nanoparticle suspension or the mixture of nanoparticle and selected pore former, 2) water removal via vacuum filtration and 60 °C drying, 3) application of cold isostatic pressing (CIP), 4) heat treatment at 900 °C (for 30 min), and 5) granulates grinding and sieving.

2.3 Fabrication of Oxygen Carrier material: Cu oxide supported on porous silica granulate

To obtain active Cu oxide supported on porous silica granulate, $\text{Cu}(\text{NO}_3)_2$ (Sigma-Aldrich) was selected as the precursor for Cu^{2+} ions and ‘dry impregnation’ method was employed. Because of the hydrophobic characteristic of the surface of silica granulate, instead of water, methanol was selected as the solvent to dissolve the precursor $\text{Cu}(\text{NO}_3)_2$ and precursor solutions with two different concentrations are prepared: 1.5 mol/L (N) and 3.0 mol/L (N). To carry out the dry impregnation process, granulates were first treated at 120 °C overnight to remove the adsorbed water inside the pores, and transferred onto a filter paper (Whatman, CAT No. 1440-090) for impregnation (step 1); the precursor solution was then added onto the granulates immediately in drop-wise orders until the adsorption reached saturation and extra solution started spread along the filter paper (step 2). Afterwards, the impregnated granulates were put back to 120 °C dryer for 2 hours (step 3), and then calcinated at 850 °C for 60 min, with a ramping speed of 5 °C/min and a stay at 550 °C for 30 min. The loading amount of Cu oxide was characterized by the mass increase on silica granulate (after calcination). To get a higher loading amount, granulates were impregnated with 3.0 mol/L $\text{Cu}(\text{NO}_3)_2$, and steps (1) to (3) were repeated once.

2.4 Chemical Looping Test on the developed Cu oxide based Oxygen Carriers

In the chemical looping combustion applications, the performance of oxygen carrier materials is characterized by their oxygen transport/conversion ability (capacity, rate) and self-regeneration

behavior from repeated reduction to oxidization cycles. With the developed oxygen carrier granulates, we investigated their performance by looking into the mass loss and mass gain of active metal oxide during the respective reduction and oxidization processes via the employment of a thermal-gravimetric analyzer (TGA, Netzsch STA 409 C/CD). Diluted CO (10 vol.% CO and 90 vol.% N₂) was taken as the reducing atmosphere and synthetic air was taken as the oxidizing and regenerating condition. The oxygen conversion capacity is calculated in the form of mass loss within each loop, that is, the mass difference between the fully oxidized phase and fully reduced phase, shown in Equation 1:

$$\text{Mass loss} = \frac{m_{\text{oxidized}} - m_{\text{reduced}}}{m_{\text{oxidized}}} * 100\% \text{ (Equation 1)}$$

To calculate the conversion rate within a single cycle, the time for the oxidizing or reducing process has to be considered and the calculation is expressed as follow:

$$\text{Conversion rate, } \alpha_{ox} = \frac{m - m_{red}}{m_{ox} - m_{red}} \text{ (Equation 2)}$$

$$\text{Conversion rate, } \alpha_{red} = \frac{m_{ox} - m}{m_{ox} - m_{red}} \text{ (Equation 3)}$$

Where, α_{ox} and α_{red} are the oxygen carrier conversion rate during oxidization and reduction process, respectively. m_{ox} and m_{red} are the mass of fully oxidized and fully reduced phases, m is the actual oxygen carrier mass loaded in the test setup.

2.5 Characterization Methods

Particle size distribution

The size of particles dispersed in water (agglomerations) were characterized by laser scattering (Beckman Coulter LS230, with laser wavelength 750 nm) and for well dispersed particles, dynamic light scattering (DLS, Zetasizer, Malvern Instruments) was employed to measure their size distribution.

Granulates porous characteristics

Granulates porous characteristics were evaluated by a mercury intrusion porosimeter (MIP, Pascal 140/440, Thermo Fisher). With this technique, an external pressure will assist the mercury to intrude into available open pores – the larger the pressure, the smaller the pores mercury can

be intruded into. The relationship between applied pressure and pore radius can be described by Washburn equation (Equation 4):

$$\rho = \frac{2\sigma \cos \theta}{\gamma} \quad (\text{Equation 4})$$

σ is surface tension, set as 0.48 N/m, θ is wetting angle, set as 140° , ρ is pressure, γ is pore radius.

Granulates microstructure

The morphology and surface microstructure of granulates were elaborated by scanning electron microscopy (NANOSEM 230 FEI, detector TLD). To avoid the charging problem, granulates were attached onto conductive carbon black substrate and a layer of Au (20 mA, 60 s) was sputtered on top of them. During the imaging time, applied high voltage is 3 kV.

Granulates Crushing force

Crushing force measurements were performed on single granulates by digital force gauges (FGP-2, Shimpo) with a resolution of 0.001 N. For each sample, the crushing force test was done with at least 40 randomly picked granulates. The mean crushing strength was calculated according to Weibull statistics, with confidence interval as 0.95.

Phase composition

X-ray diffraction analyses were carried out to detect the phase composition of as-formed oxygen carrier phase. The measurements were done by using a PANalytical diffractometer (X'Pert Pro PW3040) equipped with Ni-filtered $\text{CuK}\alpha$ -radiation ($\lambda = 1.5406 \text{ \AA}$).

3. Results and Discussion

The strategy we proposed in this work can be classified into the so called 'bottom-up' approach, with silica nanoparticle as the basic building block and micrometer scale granulates (315-500 μm) as the processed products. Efforts have been invested to break down the agglomeration of nanoparticles into well dispersed ones and tune the organization/assembly of nanoparticle units when building them up into granulates. Besides, to enhance the mechanical stability of the prepared granulate, the technique of cold-isostatic pressing (CIP) was also integrated into the procedure, as illustrated in Figure 1. This combined process was expected to offer the possibility

to tune granulate microstructure into the one with varied pore size distributions, while enhance granulates mechanical strength through the employment of CIP.

3.1 Nanoparticle agglomeration breakage

The purchased silica nanoparticles are 20 nm in diameter (supplier data), in the form of dry powders. When disperse the nanoparticles in water, agglomerations were however formed, in the size of micrometer range, as shown in Figure 2 a). In order to break down these big agglomerations, two different approaches have been applied in this work, the modification of dispersion pH and the employment of mechanical force such as vibrational ball milling and ultrasonication bath treatment. Results in figure 4 b) and c) indicate that, pH modification is not effective in breaking big agglomeration into well dispersed nano units, and the size remained unchanged in the micrometer range, while mechanical force treated samples show average sizes at ca. 45 nm, indicating the original agglomerations were successfully broken down into almost primary particle size. Additionally, the mechanical force treated suspensions are rather stable (under stirring) and comparable results could be obtained again after 24 hours stay. Therefore, for the preparation of porous silica granulates, all the prepared dispersions were treated under ultrasonication bath for 30 minutes before transferring them to next step.

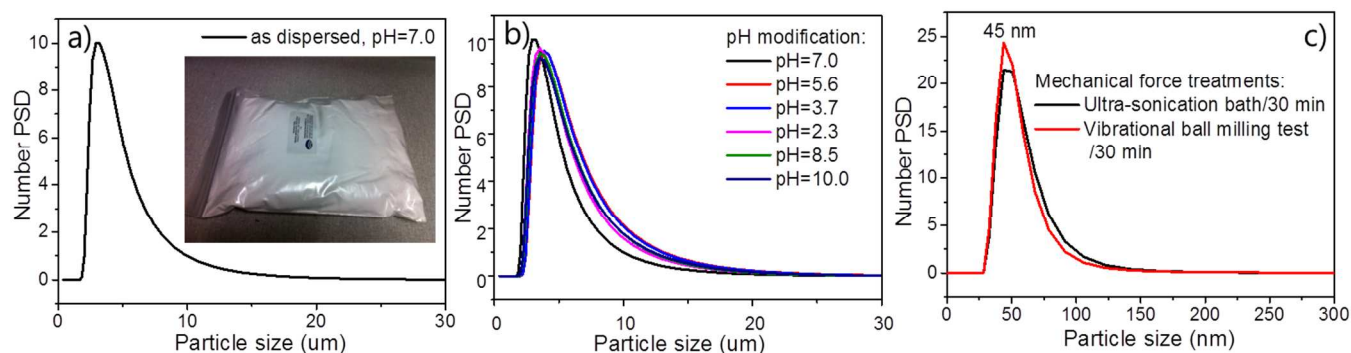


Figure 2. Picture of the as received powders and the agglomeration size in water (a), particle size after the modification of dispersion pH value (b), and (c) particle size with the employment of mechanical force.

3.2 Preparation of porous Silica granulate

3.2.1 Granulates prepared from Silica Nanoparticles

To build up porous silica granulates, we started the strategy first with pure nanoparticles. The tuning of granulates microstructure was carried out via modification of water/moisture contents in the intermediate green bodies, which was realized by controlling the drying time at 60 °C after the vacuum filtration (second step in Figure 1). With this method, green bodies with four different moisture contents were obtained: 75 wt.% (without further drying), 55 wt.% (30 min at 60 °C), 15 wt.% (60 min at 60 °C) and 7.7 wt.% (overnight stay at 60 °C). And then, each of these green bodies was divided into two parts, one for the application of CIP 50 MPa and the other one as reference (no CIP).

The resulted variations on granulate microstructure characteristics as well as crushing strengths were demonstrated in Figure 3. As noticed, for green bodies with moisture contents 15 wt.% or above, granulates pore size distributions were not really changed by the variation of moisture contents, they all shared single wide distribution with the peak value at ca. 55 nm. The application of CIP 50MPa did not bring any observable changes compared with granulates without the application of CIP. The specific pore volumes only slightly decreased, and pore size remained roughly the same. Similar trend was also noticed for the measured crushing strength values in Figure 3 c). These results indicate that, for samples with water contents above 15 wt.%, the water (non-pressable) is over saturated (75 wt.%) or in the state of saturation and upon application of CIP pressure, it was either partially squeezed out or moving from one ‘location’ to randomly another, and therefore, hardly any changes could be made on granulates’ final microstructure. However, for green bodies with a lower moisture content (7.7 wt.%, under saturation), the use of CIP 50 MPa resulted in clear changes both on the mechanical crushing strength and microstructure. More specifically, the crushing strength increased from 1.35 N to 2.49 N, while specific pore volume was reduced ca. 44%, pore size shifted to smaller range with a much sharper distribution, and peak value changed from ca. 55 nm to the mesopore range (ca. 29 nm). These changes were also confirmed by the morphology variations in the top view SEM images. Comparing the image in figure 3 d) with e), we noticed that big non-regular pores were basically all squeezed out under CIP application, and only small pores with similar sizes were obtained, fitting well with the results obtained from MIP (Figure 3 a) and b)).

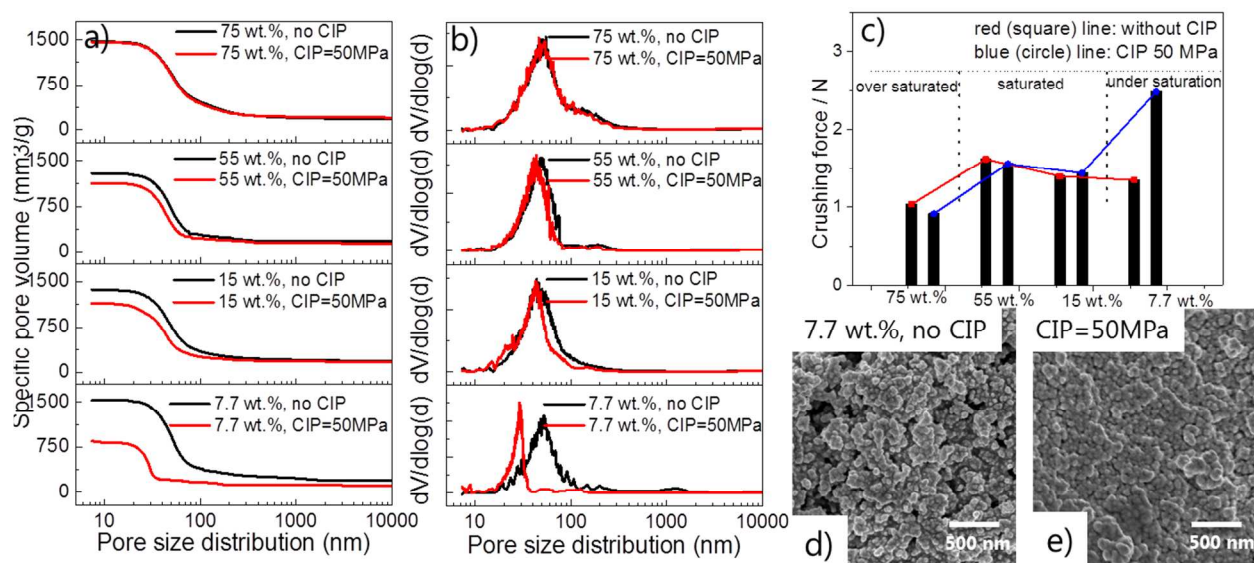


Figure 3. Granulates fabricated from silica nanoparticles—resulted changes from the application of CIP 50 MPa on green bodies with different moisture contents: a) specific pore volume, b) pore size distribution, c) mechanical crushing strength, d) top view SEM images for 7.7 wt.% moisture content green body prepared granulates (no CIP), and e) CIP 50 MPa.

It is not difficult to simulate granulate formation process from these analyses, which was illustrated in Figure 4 a). During granulate fabrication process, nanoparticles in the suspension exist in the form of small nano clusters (40-60 nm, as supported by nanoparticles' size distributions after 30 min ultra-sonication bath treatment, Figure 2 c)). It is worth to point out that, the interaction within these nanoparticle clusters are supposed to be rather strong, since they overcame the effect of ultra-sonication bath treatment, and we call them as elementary units. During the vacuum filtration and specially the drying procedure at 60 °C, water was removed and these elementary units will be brought closer (packing) to form secondary units, that is, agglomerations of nanoparticle clusters. Among the secondary units, drying process induced capillary force will cause the self-organization of the elementary units and formation of big pores, which are larger than the pores formed among elementary units. Upon the employment of CIP 50 MPa, the big pores among second units will be squeezed out easily and only the small ones will be left over, as for the situation in 7.7 wt.% moisture contained granulate formation.

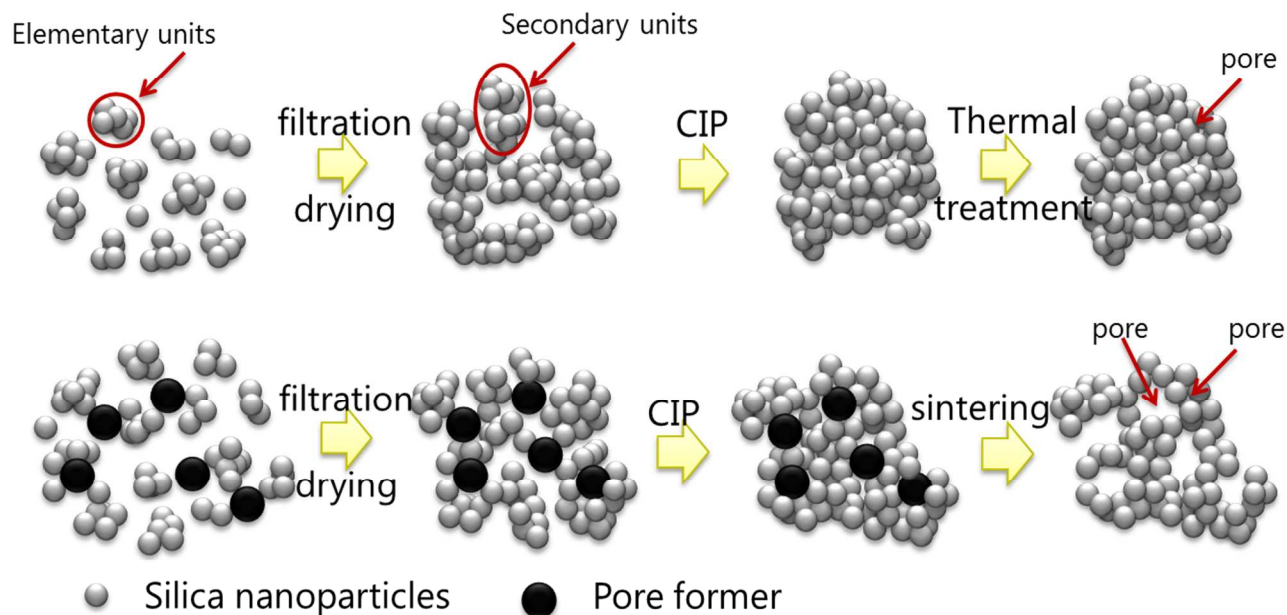


Figure 4. Schematic illustration of granulate formation process from the organization of nanoparticles: a) without pore formers and b) with pore formers, both with low moisture content.

3.2.2 Granulates prepared from Silica Nanoparticles and Pore Formers

Based on this strategy, we proposed to integrate pore formers into the nanoparticle system, to achieve granulates with a varied pore size distribution (combination of mesopores and macropores). Here, the pore formers are expected to offer some kind of spacer to withstand CIP pressure and create extra pores in addition to the ones formed among nanoparticle clusters. As illustrated in Figure 4 b), at the beginning of the fabrication process, pore formers are mixed together with nanoparticle clusters homogeneously in the suspension and then after the vacuum filtration and drying procedure, CIP 50 MPa will be applied. Similarly with non-pore former added situation, the capillary force induced big pores will be removed. However, because of the addition of pore formers, a second pore size is still expected to be generated and present. In this work, two different pore formers have been selected: 1) block copolymer Pluronic F127 and 2) high pressure (200 MPa) treated carbon black. Pluronic F127 is the ‘soft’ pore former, soluble in water, and exists in the form of monomers or aggregates depending on the environment, while carbon black is quite ‘hard’ and more resistant to pressure. Green bodies with these two pore formers have been preserved overnight at 60 °C and their water contents are very low (under

saturation). Changes on granulates structural characteristic as well as mechanical crushing strength before and after the use of CIP 50 MPa are presented in Figure 5.

As expected, the integration of pore formers (both Pluronic F127 and carbon black) clearly increased the specific pore volume and surface area compared with no pore former integrated granulates (7.7 wt.% as reference), for granulates fabricated without and with the application of CIP 50 MPa. For example, upon the application of CIP 50 MPa, the specific pore volume increased ca. 13.5 % from the contribution of F127 integration, ca. 28.4% from the contribution of Carbon black integration. Comparing with Peterson's work of using β -SiC as the precursor for SiO₂ support [20], the achieved granulate pore volume here is at least 15 times higher and surface area is 10 times higher. Besides, the integration of pore formers also brought changes on the open porosity and pore size distributions of granulates microstructure comparing with reference sample (7.7 wt.%) under CIP 50 MPa. That is, the open porosity increased from 63 % to 69 % and 71 % for F127 and Carbon black integrated granulates, respectively. For the pore size distributions, in addition to the main peak at ca.55 nm, a second pore size peaked at ca. 175 nm appeared for granulates prepared without the use of CIP 50 MPa. After the use of CIP, the obvious bi-modal pore size distribution still exists in F127 integrated granulates, but is absent in granulates with Carbon black. We assume the difference between Pluronic F127 and Carbon black could be due to Carbon black's strong resistance towards CIP pressure – the relative motion between Silica phase and Carbon black was expected and phase separation was generated, therefore, the pore former effect disappeared. While for the soft polymer Pluronic F127, it will remain together with nanoparticle agglomerations and the main expectation upon the use of CIP pressure is the volume shrinkage, and thus pore former effect can still be recognized. For F127 integrated granulates, porous structure with a combination of mesopore and macropores was obtained, and this characteristic was also demonstrated from top view SEM images in Figure 5 d), where F127 integrated granulates show pores with varied sizes.

As part of our proposed strategy, the employment of CIP, aimed to improve granulate mechanical strength, was proved effective for granulates even with the integration of pore formers, as is shown in Figure 5 c), from 0.45 N to 1.94 N for granulates with F127, and 0.32 N to 1.18 N for granulates with Carbon black. Strong mechanical strength is a crucial factor for the use of oxygen carrier materials, and a thumb rule for the selection of attrition resistant oxygen carriers for fluidized bed reactors is that the crushing force of developed granulates should be above 1 N. As

a result, we can say that the use of CIP in this work is of help to produce usable porous granulates. Comparing with the results reported in the recent publication by Song [24], the crushing force of CuO supported on silica was ca. 1.2 N after sintering at 950 °C for 6 hours, while from Ryden's investigation [18], crushing force of CuO supported on many different supports was improved to above 1 N only after increasing the sintering temperature from 950 °C to 1100 °C (4 hours), which is higher and longer than the sintering condition (850 °C for 1 hour) in this work.

By far, with the obtained results, we can then claim that, the proposed strategy, integration of pore former and the employment of CIP technique at the presence of pore former, can successfully tune the organization of nanoparticle units and enable us to build hierarchically structured porous granulates with enhanced mechanical stability. Concerning granulates bi-modal pore size distribution and higher crushing force, obviously, F127 integrated granulates hold better promises than carbon black integrated ones for the application as support to prepare oxygen carriers.

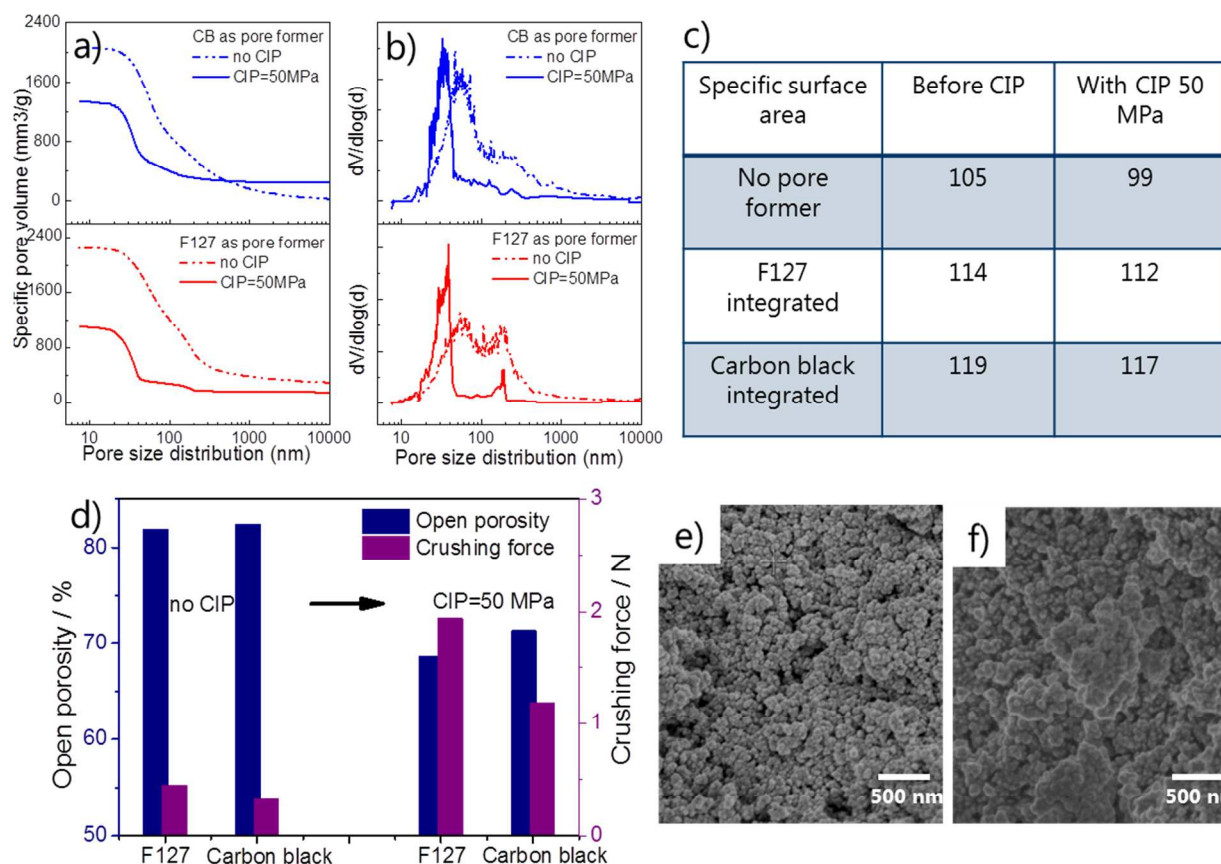


Figure 5. Granulates fabricated from Silica Nanoparticles and pore former Pluronic F127 and Carbon black: a) specific pore volume, b) pore size distribution, c) specific surface area by MIP,

d) mechanical crushing strength, e) top view SEM images for F127 integrated granulates and f) Carbon black integrated granulates, both with CIP 50 MPa, scale bars in both images are 500 nm.

3.3 Application as support for Cu Oxide and the Chemical Looping test

Wet impregnation is an often used method to load porous supports with oxygen carriers [8, 26, 28], however, for copper oxide based oxygen carrier material, Cao et.al found that it is difficult for copper precursors to penetrate into moisture filled porous structures of the supporting substrate and thus they proposed a ‘dry’ impregnation method [29]. Its main difference from wet impregnation method is the pre-treatment of porous granulate, with the aim to remove adsorbed water inside the porous structure. In our work, this dry impregnation method was taken to carry out the impregnation process. Granulates prepared from the integration of pore former F127 and under the CIP pressure 50 MPa were selected as the supports. They were pre-heated overnight at 120 °C before the impregnation process and then precursor solution $\text{Cu}(\text{NO}_3)_2$ (1.5 N and 3.0 N in methanol) was added onto the surface of pre-heated granulate. The obtained loading amount is 13 wt.% (sample I) and 30 wt.% (sample II), respectively, and the examined phase is the same for them, both with fully oxidized CuO (Figure 6).

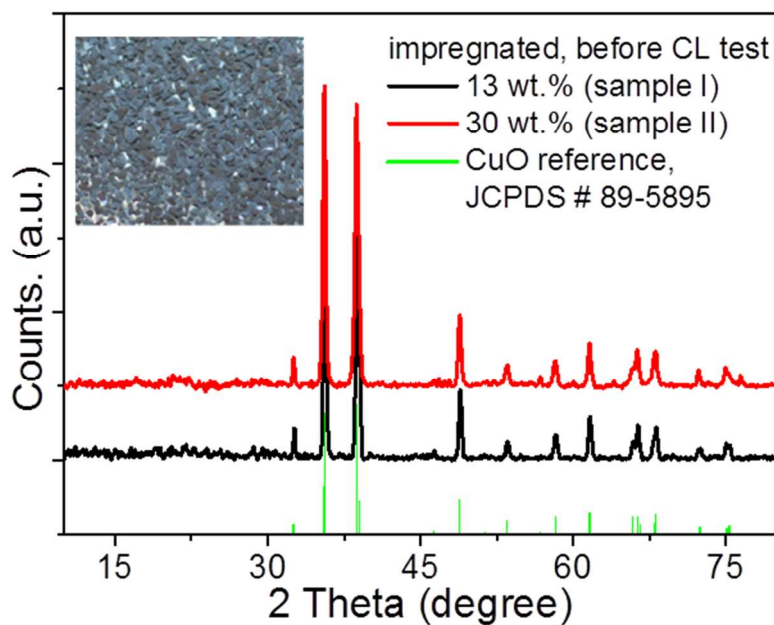


Figure 6. X-Ray diffraction pattern of Cu oxide supported on F127 integrated porous Silica granulates, impregnated by two different precursor concentrations and treated at 850°C.

Mercury intrusion porosimetry (MIP) measurement results (Table 1) reveal that after the impregnation process, both the pore volume and specific surface area decreased. For samples with a lower loading amount (13 wt.%, sample I), specific pore volume decreased from 955 mm³/g to 753 mm³/g and specific surface area decreased from 114 mm²/g to 87 mm²/g, respectively. However, for sample with a higher loading amount (30 wt.%, sample II), neither the pore volume nor surface area decreased linearly further as expected, which probably indicates a different dispersion of Cu Oxides on the surface of porous support. Moreover, top view SEM images of impregnated samples show that, the surface of 13 wt.% loaded sample presents mainly the homogeneous dispersion of small nanoparticles (Figure 7 a) and b)), while 30 wt.% loaded sample show additionally the obvious presence of large micrometer units (Figure 7 c)).

Table 1. Pluronic F127 integrated silica granulates (CIP 50 MPa): porous characteristics change before and after the impregnation process

Parameters	Cu oxide loading amount / %	Specific Pore volume / mm ³ /g	Specific surface area mm ² /g	Open porosity / %	Crushing force / N
no	---	955	114	68.7	1.94
13 wt.% (sample I)	13.3	753	87	65.4	1.82
30 wt.% (sample II)	30.2	709	80	64.9	1.75

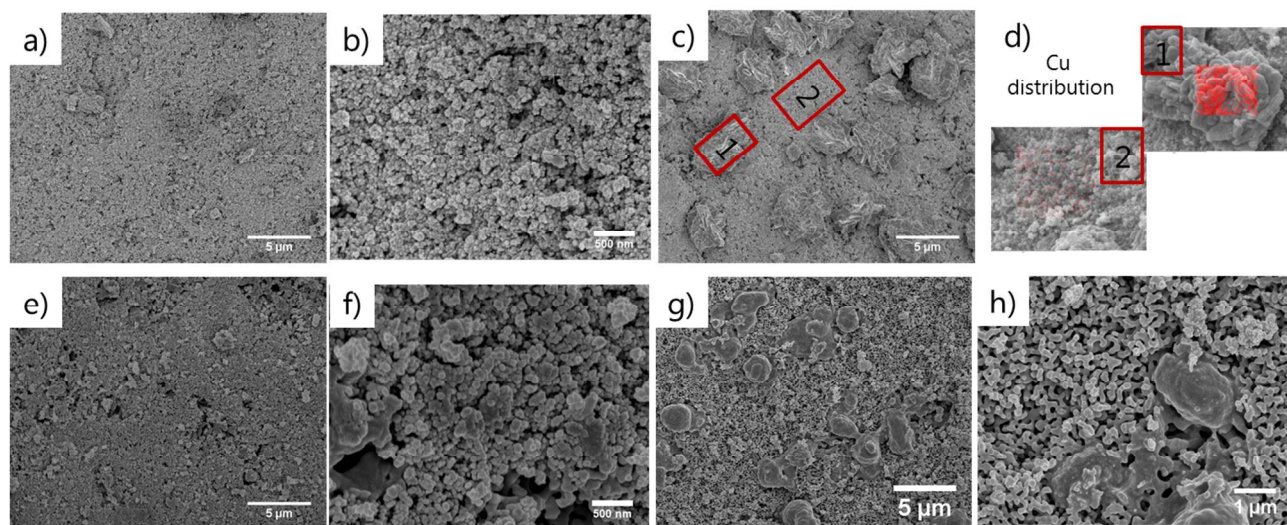


Figure 7. TOP view SEM images of Cu oxide supported on F127 integrated porous silica granulates before the multiple looping tests: a) and b) for 13 wt.% loaded sample, c) for 30 wt.% loaded sample and d) selected area elemental distribution (Cu); after 11 looping cycles: e) and f) for 13 wt.% loaded sample, g) and h) for 30 wt.% loaded sample.

To check the performance of developed Cu oxide based oxygen carrier in chemical looping process, we have carried out the test in a simplified fixed bed reactor setup, by taking diluted CO (10 vol.% CO and 90 vol.% N₂) as combustion fuel (reducing atmosphere) and synthetic air as regenerating atmosphere (oxidizing). The tests were performed at the constant temperature 850°C, and the running time was set enough to finish 11 cycles. The reducibility and regeneration ability of CuO, presented by the loss and re-gain of oxygen atoms, were characterized by mass loss or mass gain in the thermal gravimetric analyzer (TGA). The results were shown in Figure 8 a).

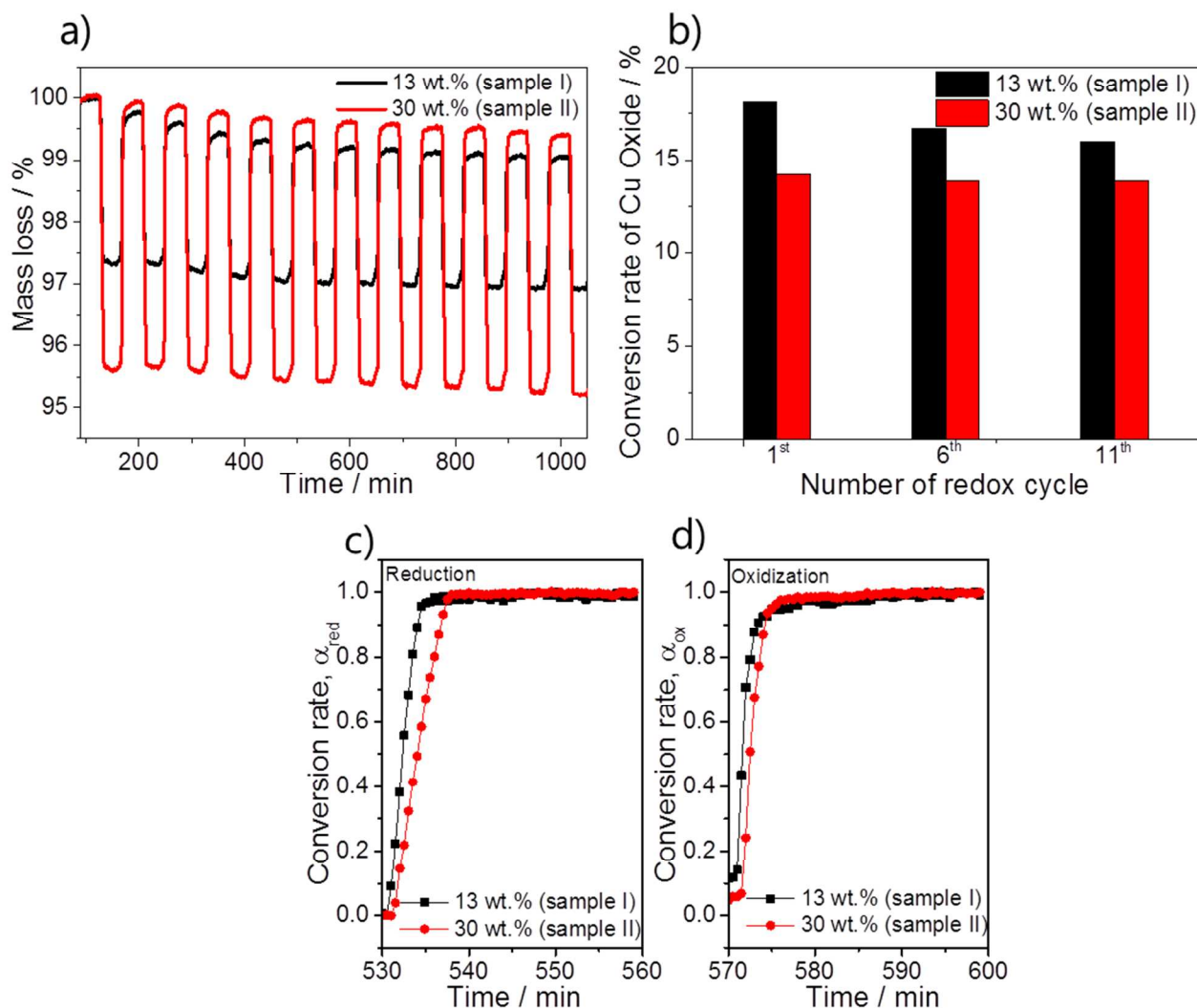


Figure 8. Results of Chemical looping tests: a) mass loss curves for CuO supported on F127 integrated porous Silica granulates, b) conversion rate of CuO during the 1st, 6th and 11th cycles, c) reduction rate and d) oxidization rate during the 6th looping cycle. The Values in figure b) are calculated via dividing the oxygen transport capacity by the amount of CuO loading.

The oxygen transport capacity is presented in the form of samples' mass loss during the looping test (Figure 8 a)). For the fabricated CuO based oxygen carriers, an oxygen transport capacity of 4.3 % was shown for 30 wt.% loaded sample, while 2.4 % for 13 wt.% loaded sample. For the same CuO/SiO₂ system (preparing from different methods), Song [2, 24] and Peterson [20] also studied the performance of their developed oxygen carriers, and the comparison on the oxygen transport capacity was shown in Table 2. As can be seen, even with lower loading amounts, oxygen carriers developed in this work achieved similar or even higher level of oxygen transport

capacities comparing with the counterparts' higher loaded samples, e.g., 13 wt.% loaded sample vs. 18 wt.% in Song's work, 30 wt.% loaded sample vs. 40 wt.% or 49.8 wt.% in Peterson's and Song's work. This indicates that, the CuO loaded onto the developed hierarchical structured porous silica granulates in this work shows higher conversion efficiency than the referred others, which should be accounted to the favored porous characteristics of the developed support granulates.

Table 2. Oxygen transport performance of CuO oxygen carriers supported on Silica

References	CuO loading amount	Operation temperature	Oxygen transport capacity	Conversion rate of Cu Oxide ^a
This work	13 wt. %	850 °C	2.4 %	18.1 %
Song [24]	18 wt. %	850 °C	ca. 1.8 %	10 %
This work	30 wt. %	850 °C	4.3 %	14.2 %
Peterson [20]	40 wt. %	900 °C	ca. 4.6 %	11.5 %
Song [2]	49.8 wt. %	850 °C	ca. 5 %	10 %

^a Values are calculated via dividing the oxygen transport capacity by the amount of CuO loading.

Besides, in Figure 8 b), we take the loading amount of CuO into consideration and calculate the absolute conversion rate of loaded CuO, 18.1 % for sample I where CuO was mainly composed of small nanoparticles, while 14.2 % for sample II where CuO contained large bulk units. Since the theoretical conversion rate for converting CuO to Cu is 20% (the lost one oxygen atom divided by the mass of CuO: 16/80) and 10% for converting CuO to Cu₂O, the situation here was the mixture of these two reactions, just as noticed from porous diatomite supported CuO oxygen carrier materials[30]. Obviously, it could be calculated that, for small nanoparticles composed CuO in sample I, the loaded CuO was largely converted to fully reduced phase Cu (80% for the 1st cycle, for example), while for large bulk units composed CuO in sample II, only 40% was converted to Cu and the rest 60% was converted to intermediate state Cu₂O. As for the change of CuO conversion rate from cycle 1 to cycle 11, in sample I, the size of small nanoparticles was somehow increased, which could be responsible for its slight decrease in Figure 8 b). For sample II, the micrometer units showed no hints of agglomeration, instead of that, their shapes were shown to be rounded and the size was decreased (Figure 7c versus 7g). This effect can be

attributed to pre-sintering effect during the cycling process and is well known for pure copper particles after first or second CLC cycle. However, the conversion rate of CuO was rather stable for this sample, as seen in Figure 8 b).

Moreover, taking the result of cycle 6th as an example, we went a step further and calculated the reaction rates during both the reduction and oxidization periods, by taking the reduction or oxidization time into consideration. From the curves in Figure 8 c) and d), we can see that the reaction rate, specially the reduction rate, is rather faster for CuO in the form of well dispersed small nanoparticles (sample I) than the one with large units (sample II). These results indicate that, the conversion rate is higher (sample I's and sample II's slope comparison in c) and d)) and the reaction is faster if CuO was presented in the form of small nanoparticles. As have been studied by [31-33], the 'chemical reaction' between CuO and Cu or Cu₂O are not limiting steps in the process, therefore, oxygen diffusion is the contributing factor to the differences we noticed here. Clearly, oxygen diffusion in micrometer units should take longer time than in small nanoparticles, thus the average reaction time is longer and reaction rate is slower.

4. Conclusion

Porous granulates are highly required as supports of oxygen carrier materials for the application in chemical looping process, to capture CO₂ emission from fossil fuel powered plants. In this work, to achieve porous granulates with a hierarchical structure and enhanced mechanical stability, a bottom-up approach was employed, with silica nanoparticles as basic building blocks and large micrometer range (315 μm to 500 μm) granulates as the final products. To realize these goals, organization of silica nanoparticles and employment of cold isostatic pressing (CIP), as two main tricks, have been integrated into granulate fabrication strategy.

Organization of silica nanoparticles requires the breaking of nanoparticle agglomerations into small nano units, and the employment of mechanical force treatments (ultra-sonication bath or vibrational ball milling) ensure to break 3-5 μm agglomerations into nano units at ca. 45 nm. To tune the organization of these well dispersed nano units under the application of cold isostatic pressure, moisture contents in the vacuum filtration generated green bodies have to be maintained in a very low level (under saturation state). Based on this, we managed to integrate soft pore

former Pluronic F127 into the nanoparticle system and achieved granulates with desired properties: mesopore (ca. 33 nm) and macropore (ca. 175 nm) combined hierarchical porous structure, high pore volume ($955 \text{ mm}^3/\text{g}$) and surface area ($114 \text{ mm}^2/\text{g}$), as well as enhanced crushing force 1.94 N.

Finally, via the dry impregnation method, fully oxidized CuO was loaded on the surface of porous granulates. A loading amount of 30 wt.% was obtained after repeating the impregnation process only twice. Further simulated chemical looping tests revealed that, the CuO supported on developed silica granulate shows a higher oxygen transport efficiency comparing with reference work. However, more work has to be done to further improve the performance of developed oxygen carrier in this work, such as the optimization of impregnation process to achieve a higher loading amount of CuO. Nevertheless, the strategy we proposed to fabricate mechanical stable porous granulates should be not only interesting for oxygen carriers in chemical looping process, but also for other kinds of high temperature used catalysts.

Acknowledgement

This work is financially supported by the Competence Center Energy and Mobility (CCEM) research program of Switzerland. Dr. Yujing Liu is thankful to the support of EMPA Marie-Curie Postdoc fellowship and the authors appreciate the help from Dr. Lassi Karvonen on the measurement of multiple cycle chemical looping test.

Reference

1. Buhre, B.J.P., et al., *Oxy-fuel combustion technology for coal-fired power generation*. Progress in Energy and Combustion Science, 2005. **31**(4): p. 283-307.
2. Song, H., et al., *Reactivity of Al₂O₃- or SiO₂-Supported Cu-, Mn-, and Co-Based Oxygen Carriers for Chemical Looping Air Separation*. Energy & Fuels, 2014. **28**(2): p. 1284-1294.
3. Adanez, J., et al., *Progress in Chemical-Looping Combustion and Reforming technologies*. Progress in Energy and Combustion Science, 2012. **38**(2): p. 215-282.
4. *Clean Coal' Technologies, Carbon Capture & Sequestration*. <http://www.world-nuclear.org/info/Energy-and-Environment/-Clean-Coal--Technologies/>, 2015.
5. Romeo, L.M., et al., *Integration of power plant and amine scrubbing to reduce CO₂ capture costs*. Applied Thermal Engineering, 2008. **28**(8-9): p. 1039-1046.
6. Booth, N., *Amine scrubbing for CO₂ capture from power plant flue gas*. http://www.rsc.org/images/Booth-2007_tcm18-102752.pdf, 2007.
7. van Garderen, N., *Development of a new type of highly porous oxygen carrier support for fluidized bed reactors*. 2012.
8. Qilei, S., et al., *A high performance oxygen storage material for chemical looping processes with CO₂ capture*. Energy & Environmental Science, 2013. **6**(1): p. 288-98.

9. Lyngfelt, A., *Chemical-looping combustion of solid fuels - Status of development*. Applied Energy, 2014. **113**: p. 1869-1873.
10. Lyngfelt, A., et al., *A fluidized-bed combustion process with inherent CO₂ separation; application of chemical-looping combustion*. Chemical Engineering Science, 2001. **56**(10): p. 3101-3113.
11. Adanez, J., et al., *Selection of oxygen carriers for chemical-looping combustion*. Energy & Fuels, 2004. **18**(2): p. 371-377.
12. Gayan, P., et al., *Effect of Support on the Behavior of Cu-Based Oxygen Carriers during Long-Term CLC Operation at Temperatures above 1073 K*. Energy & Fuels, 2011. **25**(3): p. 1316-1326.
13. de Diego, L.F., et al., *Development of Cu-based oxygen carriers for chemical-looping combustion*. Fuel, 2004. **83**(13): p. 1749-1757.
14. van Garderen, N., et al., *Influence of porous substrate on copper based oxygen carrier efficiency for chemical-looping combustion*. Microporous and Mesoporous Materials, 2014. **190**: p. 362-370.
15. van Garderen, N., et al., *Improved gamma-alumina support based pseudo-boehmite shaped by micro-extrusion process for oxygen carrier support application*. Ceramics International, 2012. **38**(7): p. 5481-5492.
16. Corbella, B.M., et al., *Characterization and performance in a multicycle test in a fixed-bed reactor of silica-supported copper oxide as oxygen carrier for chemical-looping combustion of methane*. Energy & Fuels, 2006. **20**(1): p. 148-154.
17. Adanez-Rubio, I., et al., *Development of CuO-based oxygen-carrier materials suitable for Chemical-Looping with Oxygen Uncoupling (CLOU) process*. 10th International Conference on Greenhouse Gas Control Technologies, 2011. **4**: p. 417-424.
18. Ryden, M., et al., *CuO-Based Oxygen-Carrier Particles for Chemical-Looping with Oxygen Uncoupling - Experiments in Batch Reactor and in Continuous Operation*. Industrial & Engineering Chemistry Research, 2014. **53**(15): p. 6255-6267.
19. Zhang, Y., et al., *Influence of Porosity on Performance of Freeze-granulated Fe₂O₃/Al₂O₃ Oxygen Carriers Used for Chemical Looping Combustion* Energy and Environmental Research, 2012. **2**(1): p. 12.
20. Peterson, S.B., et al., *Characteristics and CLOU Performance of a Novel SiO₂-Supported Oxygen Carrier Prepared from CuO and beta-SiC*. Energy & Fuels, 2013. **27**(10): p. 6040-6047.
21. Su, B.L., et al., *Hierarchically Structured Porous Materials: from Nanoscience to Catalysis, Separation, Optics, Energy, and Life Science, first edition*. 2012.
22. Li, Y., et al., *Hierarchically Structured Porous Materials for Energy Conversion and Storage*. Advanced Functional Materials, 2012. **22**(22): p. 4634-4667.
23. Akimov, G.Y., *Cold isostatic pressing as a method for fabricating ceramic products with high physicommechanical properties*. Refractories and Industrial Ceramics, 1998. **39**(7-8): p. 283-287.
24. Song, H., et al., *Analysis on Chemical Reaction Kinetics of CuO/SiO₂ Oxygen Carriers for Chemical Looping Air Separation*. Energy & Fuels, 2014. **28**(1): p. 173-182.
25. Song, H., et al., *Development of a Cu-Mg-Based Oxygen Carrier with SiO₂ as a Support for Chemical Looping Air Separation*. Energy & Fuels, 2014. **28**(1): p. 163-172.
26. Wang, Z.L., et al., *Surface structure and catalytic behavior of silica-supported copper catalysts prepared by impregnation and sol-gel methods*. Applied Catalysis a-General, 2003. **239**(1-2): p. 87-94.
27. Mattisson, T., *Materials for Chemical-Looping with Oxygen Uncoupling*. ISRN Chemical Engineering, 2013. **2013**: p. 19.
28. Meille, V., *Review on methods to deposit catalysts on structured surfaces*. Applied Catalysis a-General, 2006. **315**: p. 1-17.

29. Cao, Y., et al., *Preparation and Characterization of Lanthanum-Promoted Copper-based Oxygen Carriers for Chemical Looping Combustion Process*. *Aerosol and Air Quality Research*, 2014. **14**(2): p. 572-584.
30. van Garderen, et al., *Development of copper impregnated porous granulates for chemical-looping combustion*. *Fuel*, 2014. **119**(0): p. 323-327.
31. Poulston, S., et al., *Surface oxidation and reduction of CuO and Cu₂O studied using XPS and XAES*. *Surface and Interface Analysis*, 1996. **24**(12): p. 811-820.
32. Goldstein, E.A., et.al., *Chemical kinetics of copper oxide reduction with carbon monoxide*. *Proceedings of the Combustion Institute*, 2011. **33**: p. 2803-2810.
33. Martinez-Arias, A., et al., *Comparative study on redox properties and catalytic behavior for CO oxidation of CuO/CeO₂ and CuO/ZrCeO₄ catalysts*. *Journal of Catalysis*, 2000. **195**(1): p. 207-216.

A table of contents entry:

One sentence text:

Via modifying the templating synthesis of hierarchical nanomaterials, a strategy was proposed to generate bi-modal porous granulates with mechanical stability.

Graphic:

